

SLAMMING COMPUTATION ON THE MULTIHULL GROUPAMA 3

Y. Roux, Company K-Epsilon, France
J. Wackers, Ecole Centrale de Nantes, France
L. Dorez, Team Groupama, France

SUMMARY

Difficulties that forced the maxi Groupama 3 to withdraw from the Jules Verne Trophy between Brazil and Africa in November 2009 showed the need for a comprehensive study of the slamming phenomenon on hull bottoms in unforeseen navigation conditions.

A survey in South Africa confirmed that structural damages were due to slamming stress on the rear of the windward hull, which has been underestimated. This condition appears in a swell when the multihull takes off and crashes back into the water at a boat speed of 30 to 40 knots.

The latest version of the software FINE™/Marine developed by CNRS, Ecole Centrale de Nantes and Numeca International allows the precise simulation of this type of problem. Indeed, the use of an automatic grid refinement algorithm enables the precise modelization of the impact of the hull on the water surface and the computation of the generated pressure field, which will be used by the designers to reinforce the structure of the hull.

We present in this paper the particularities of the automatic refinement method and its application to the trimaran Groupama 3 in the condition of the impact of the hull at an angle with respect to the sea.

1. INTRODUCTION

This paper presents the study of the impact of the bottom of a Groupama 3 float onto the sea surface. This phenomenon appears in very specific conditions where the boat is sailing in reaching conditions against a swell front. In this case the multihull jumps on the wave. The impact on the waves at every landing induces extremely high loads to the float structure and deteriorate this structure.

The numerical modelization of slamming needs a very accurate and robust unsteady hydrodynamic flow solver able to capture the deformation of the free surface during the impact. We present in this paper a new automatic adaptive grid refinement method recently developed for the software FINE™/Marine and we apply it to the multihull Groupama 3 in an extreme condition of slamming.

2. NUMERICAL METHOD

We use the software FINE™/Marine

2.1 THE ISIS-CFD RANS SOLVER AT A GLANCE

The unsteady hydrodynamic RANS equations with free surface are solved using the FINE™/Marine software. The mesh generator HEXPRESS included in FINE™/Marine offers pure-hex unstructured mesh generation allowing complex geometry meshing in affordable turn-around time.

The ISIS-CFD RANS flow solver is developed by EMN (Equipe Modélisation Numérique, the CFD Department of the Fluid Mechanics Laboratory at Centrale Nantes). Turbulent flow is simulated by solving the incompressible unsteady Reynolds-averaged Navier-Stokes (RANS) equations. The solver is based on the finite volume method to generate the spatial discretization of the transport equations. The face-based method is generalized to two-dimensional, rotationally symmetric, or three-dimensional unstructured meshes for which non-overlapping control volumes are bounded by an arbitrary number of constitutive faces. The velocity field is obtained from the momentum conservation equations and the pressure field is extracted from the mass conservation constraint, or continuity equation, transformed into a pressure equation. Free-surface flow is simulated with a multi-phase flow approach: the water surface is captured with a conservation equation for the volume fraction of water, discretised with specific compressive discretisation schemes, see [7].

In the case of turbulent flows, additional transport equations for modeled variables are discretized and solved using the same principles. Most of the classical linear eddy-viscosity based closures like the two-equation $k-\omega$ SST model by Menter [6], for instance, are implemented. Two more sophisticated turbulence models are also implemented in the ISIS-CFD solver: an explicit algebraic Reynolds stress model (EARSM) [1], and a Reynolds stress transport model [2].

The technique included for the 6 degree of freedom simulation of ship motion is described by [5]. Time-integration of Newton's laws for the ship motion is combined with analytical weighted or elastic analogy

grid deformation to adapt the fluid mesh to the moving ship.

2.2 THE REFINEMENT METHOD

Recently, an automatic grid refinement capability has been integrated in ISIS-CFD [8]. This technique is to be used on a day-to-day basis for all the different applications of the flow solver and it is supposed to evolve effortlessly as the possibilities of the solver grow over the years. Therefore, the mesh adaptation method has been made general: it is suited for unstructured grids around the complex geometries commonly treated, directional refinement is used to keep the size of 3D refined grids low, and derefinement of refined grids is included to enable unsteady flow simulation. Like the flow solver, the refinement method is fully parallel. The refinement procedure is completely integrated in the flow solver.

During a flow calculation with adaptive grid refinement, the refinement procedure is called repeatedly to keep the grid permanently adapted to the developing solution. Globally, the method works as follows: the flow solver is run on an initial grid for a limited number of time steps. Then the refinement procedure is called. If a refinement criterion, based on the current flow solution, indicates that parts of the grid are not fine enough, these cells are refined and the solution is copied to the refined grid. On this new grid, the flow solver is restarted. Then the refinement procedure is called again, to further refine or to derefine the mesh. This cycle is repeated several times. When computing steady flow, the procedure eventually converges: once the flow starts to approach a steady state and the grid is correctly adapted to this state according to the refinement criterion, then the refinement procedure keeps being called, but it no longer changes the grids. For unsteady flow, the mesh keeps changing as it adapts itself to the flow in evolution.

To ensure robustness and flexibility of the grid refinement method, it is divided into three distinct parts that exchange only minimal information. First, the refinement criterion is computed, a scalar or tensor field that indicates the local desired cell size. This criterion should be based on the flow field, it may be computerd from any quantity desired. To permit the user choice of refinement criteria and the easy incorporation of new refinement criteria in the code, the criterion does not have to take into account the type or the orientation of the cells; in general it is a smooth field variable.

Based on this criterion, the decision is taken which cells to refine or to derefine. While this decision may depend on the type of the cells, it does not depend on the specific way in which the refinement criterion is calculated. It remains the same for any refinement criterion. During the refinement decision step, the decision in each cell is adapted to its neighbour cells: to guarantee the quality of the mesh, extra cells may need to be refined, or

derefinement of cells may be prevented. At the end of the decision step, before a single cell is actually refined, the refinement for the entire grid is known.

Finally, the actual grid adaptation is performed; cells are divided into smaller cells, or existing small cells are merged back into their original large cells. Care is taken, after the treatment of each individual cell, to leave a valid mesh with all the pointers between cells, faces, and nodes in place, even if one knows that certain pointers will be changed again when a neighbour cell is refined later on. This guarantees that, when a cell is refined, it does not have to distinguish between neighbour cells that are refined, that will be refined, or that remain unchanged. The added flexibility and robustness of the code are well worth the extra work this represents. The refinement step includes automatic load balancing with the ParMETIS library [4].

As the grid refinement method mainly changes the topology of the grid, while the weighted mesh deformation technique of ISIS-CFD influences only the position of the mesh nodes, the combination of these two techniques is feasible without large modifications to any of them. Therefore, unsteady grid refinement can be performed for simulations with moving bodies, without major difficulties.

2.3 REFINEMENT CRITERION

The criterion chosen for this study refines the grid in the neighbourhood of the water surface. Directional refinement is employed to refine in the direction normal to the surface only. Where the free surface is diagonal to the grid directions, isotropic refinement is used, but where the surface is horizontal, directional refinement is chosen; the resulting zone of directional refinement includes the undisturbed water surface, as well as smooth wave crests and troughs. This is essential to keep the number of grid cells low, as the water surface is often nearly undisturbed in most of the domain. Figure 1 gives an illustration of this refinement principle.

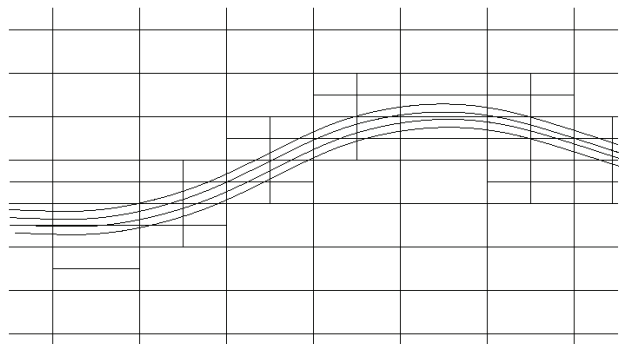


Figure 1: Isotropic and directional refinement at the free surface. The curves represent volume fraction isolines.

Directional refinement normal to the free surface implies, that the refinement criterion imposes a constraint on the cell size in that normal direction only. The cell size in all

other directions is kept as large as possible. Thus, cells that are oriented diagonally to the interface must necessarily be refined in all directions, but cells that are aligned with the interface can be refined in one direction only.

This criterion is useful to increase the precision for simulations with free-surface waves. While it is applicable for any type of wave, it is especially successful for cases where small local wave details play an important role. Thus, the simulation of slamming, which involves localised pressure peaks, is a natural field of application.

3. IMPACT STUDY OF GROUPAMA 3 FLOAT

3.1. GENERAL PRESENTATION

The impact case chosen for this study is a computation of the float with a trim angle of 2° to create the dangerous configuration with the rear part of the hull parallel to the free surface. We impose the movement of the float with an horizontal and vertical boat speed, Figure 2.

The velocities imposed in the horizontal and vertical motion correspond to the boat speed in sailing condition with a vertical motion estimated by video measurement.

For reasons of confidentiality we give the vertical velocity as a function of horizontal one:

$$U_z = -3.6 U_x$$

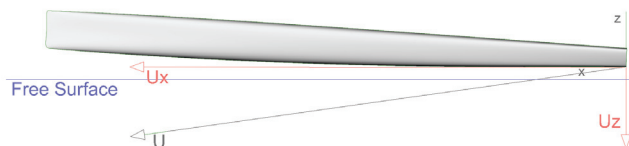


Figure 2 Geometry and frame of reference

3.2 MESH GENERATION

The mesh of the float is generated with the float positioned 0.1 m above the free surface. A full hexahedral unstructured mesh of 2 million cells has been generated using HEXPRESS on the half part of the domain. The initial mesh is pre-refined in the region of the impact (on the hull and also on the free surface at $Z=0$)

Common criteria for good boundary layer description and free surface resolution have been respected:

- The thickness of the first cell next to the wall in the boundary layer y_p is defined as function of y^+ , Reynolds number Re , friction velocity U_τ and the waterline length Lpp :

$$y_p = \frac{y^+}{Re.U_\tau} Lpp$$

The use of a law wall with $y^+ = 80$ leads to $y_p = 0.0004 \text{ m}$

- Best practice in FINE/Marine in the case of resistance computation has shown that the vertical height of the cells Dz inside the free surface region has to satisfy the following condition:

$$Dz = 0.001 Lpp$$

Figures 3 shows the detail of the mesh around the hull.

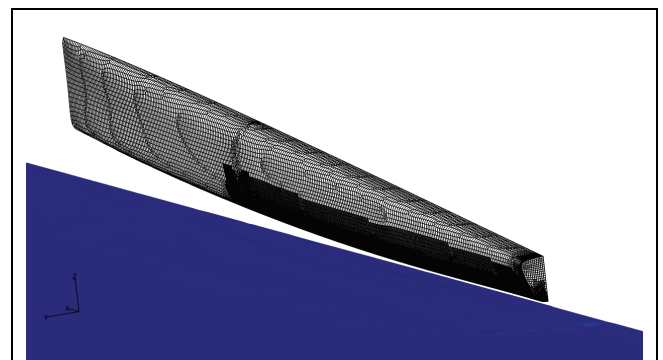


Figure 3. General view of the Gma3 hull mesh.

3.3 INPUT DATA, BOUNDARY CONDITIONS:

We present the input data and the boundary conditions for the computation:

- Boundary conditions for the volume mesh. To take into account the movement of the float, the computation is realized with an imposed motion of the volume mesh in Z direction and X direction.

The boundary conditions are:

- Velocity imposed on the front (X_{min}), back (X_{max}), and side (Y_{min}) surfaces.
- Hydrostatic pressure imposed on the bottom (Z_{min}) and the top plane (Z_{max}).
- Mirror conditions on the symmetry plane of the hull.
- Wall function on the hull surface.

- Refinement input data. For the refinement we need to specify several data. The most important of these are:

- The region near the float where the refinement will be active. This region is defined as a parallelepiped box where the refinement in X, Y and Z-direction is active. In our case we choose the size of the box as:

$$0 < X < 0.5 \text{ LPP}$$

$$0 < Y < 0.01 \text{ LPP}$$

- The threshold is the target size for the cells after grid refinement. We realized the computation with a threshold value of $DZt = 0.0002 \text{ LPP}$ with a diffusion of 2 (which means the refinement is spread out

to a zone of two cells around the cells indicated by the refinement criterion).

The refinement criterion and the limiting box combined cause grid refinement around the water surface, in a region that moves with the float, there where the thickness of the cells is superior to DZ_t .

To reduce the number of cells and the computation time, the derefinement is also active. Once refined cells are situated under the free surface they are merged back into the original coarse cells and the mesh is the same as before the refinement.

- Time step. The choice of the time step is one of the most important parameters for the modelization of slamming. The highest pressure induced by the impact appears at the very first contact between the hull and the water, the time step has to be small enough to capture this phenomenon. We choose to use a small time step which is adapted to give a constant maximum Courant number computed on the free surface. At the beginning the time step is $DT=0.001$ s and the smallest value is $DT=0.00009$ s.

4. RESULTS

For reasons of confidentiality, all the pressure values are given in non-dimensional form.

The unsteady computation describes 0,028456 s of the phenomenon. As we explained before the time step is not constant but adapted at every iteration according to the Courant number fixed to 5 for this computation.

We decomposed the impact in two phases: phase 1 [1 to 10] where the pressure increases and phase 2 [1 to 10] where the pressure decreases. We show the different data at every 4 iterations from 0.013 s to 0.025049 s. Table 1 gives the time for each item in the two phases.

Item	Time Phase 1 (s)	Time phase 2 (s)
1	0.013000	0.021642
2	0.016399	0.022026
3	0.017415	0.022406
4	0.018221	0.022798
5	0.018989	0.023139
6	0.019722	0.023488
7	0.020402	0.023841
8	0.020889	0.024222
9	0.021173	0.024627
10	0.021642	0.025049

Table 1: Time for each item in the two phases.

In the figures 4 and 5 we present the variation of the non-dimensional pressure on the hull at $Y=0$ from the transom ($X=0$ m) toward the bow ($X=12$ m).

- Phase 1. The pressure impact appears first near the transom and develops itself as a constant value between 1 and 8 meters from the transom. At the end of the phase 1, at 0.0216 s, the constant value of the pressure is around 3.
- Phase 2. We observed a decrease of the constant value pressure from 3 to 1 and an increase of local pressure induced by the impact of the keel line with the free surface. This impact is more localized and less dangerous for the structure. The value of constant pressure is reduced to one, which corresponds to the dynamic pressure of the flow on the hull.

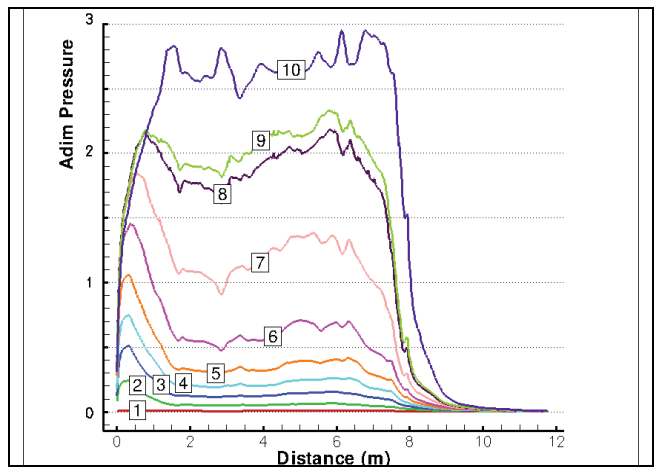


Figure 4: Evolution of the pressure at $Y=0$ from the transom ($X=0$ m) to the bow ($X=30$ m). From $T = 0$ s [1] to $T = 0.021$ s [10]

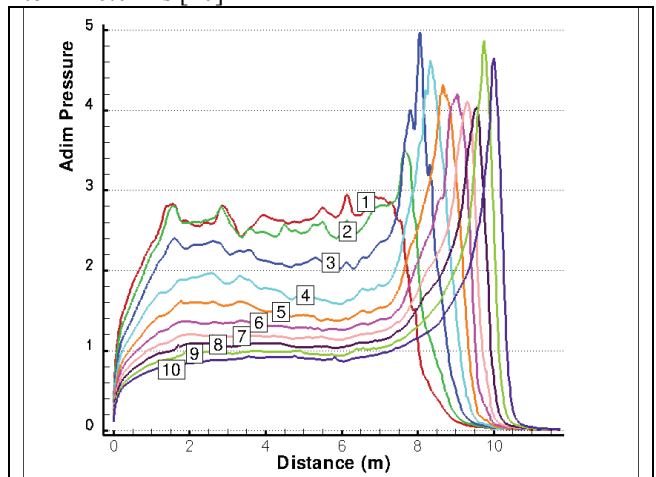


Figure 5: Evolution of the pressure on $Y=0$ from the transom ($X=0$ m) to the bow ($X=30$ m). From $T = 0.021$ s [1] to $T = 0.025$ s [10]

In the figures 6 and 7 we present for item [2, 4, 6, 8 and 10] of the two phases the non-dimensional pressure field. We observed an increase of the pressure until a constant value of a value around 3 in phase 1 and a decrease of this pressure in phase 2.

The geometrical characteristic of the zone on the hull where there is the dangerous development of the constant

pressure [8 and 10] of phase 1 is 7 m length and 0.3 m width. As we explained before, the evolution of the non-dimensional pressure peak in the phase 2 is very concentrated near the point of impact of the keel line with the free surface. The impact goes forward towards the bow until the landing of the float.

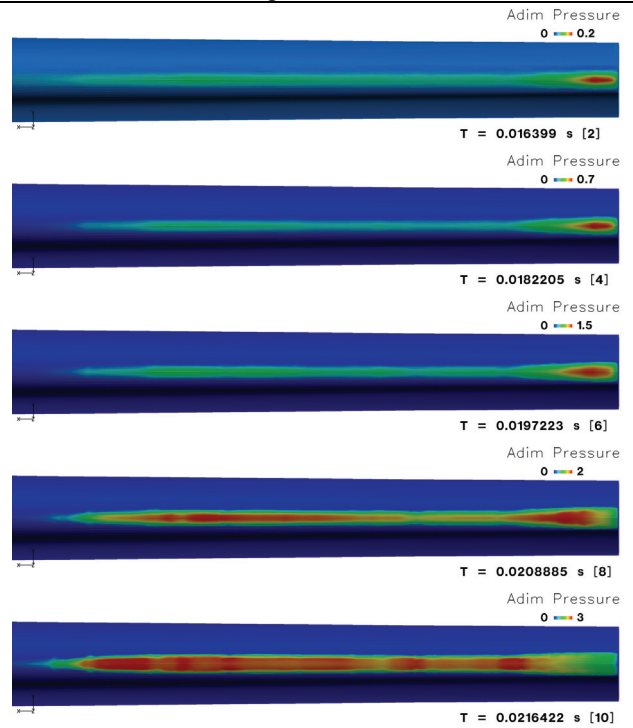


Figure 6: Field of the non-dimensional pressure on the hull, Phase 1.

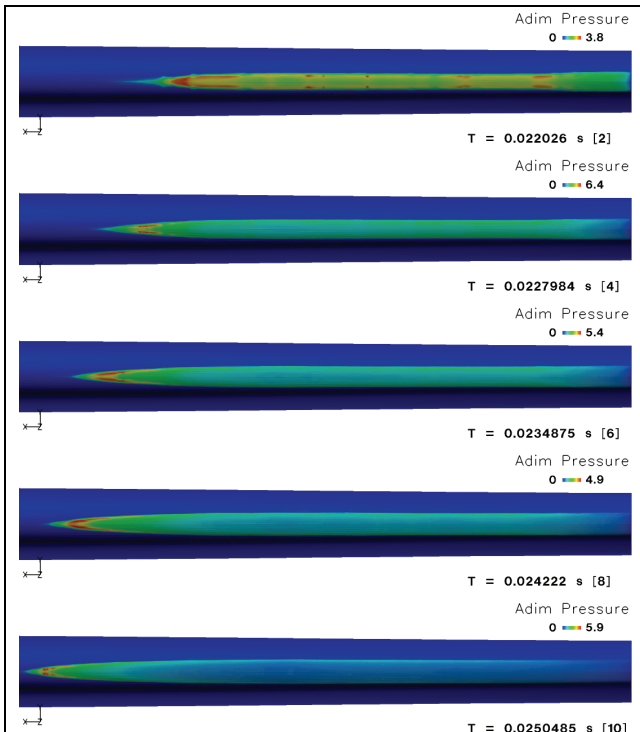


Figure 7: Field of the non-dimensional pressure on the hull, Phase 2.

In the figures 8, 9 and 10 we present an illustration of the automatic refinement methodology using for this study For the cases [2], [4], [6], [8] and [10] of the phase 1 we show the mesh section at $X = 5\text{m}$. (For a better understanding we show in each picture the hull in the same position, while the free surface is in motion).

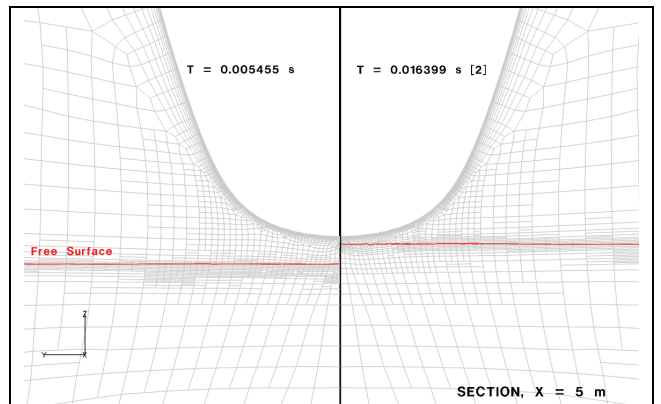


Figure 8: Mesh in the section $X=5\text{m}$, evolution of the refinement from the begining to [2] in phase 1

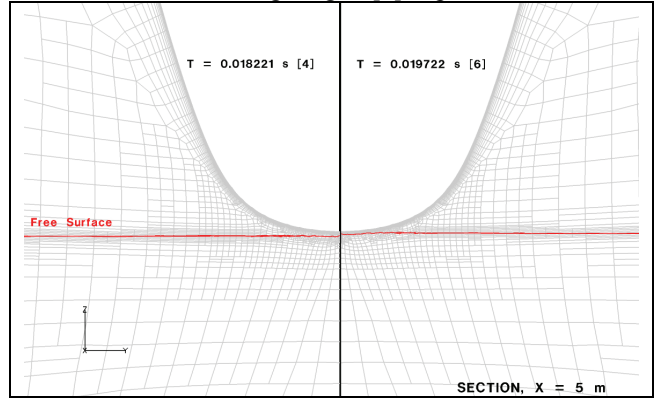


Figure 9: Mesh in the section $X=5\text{m}$, evolution of the refinement from the [4] to [6] in phase 1

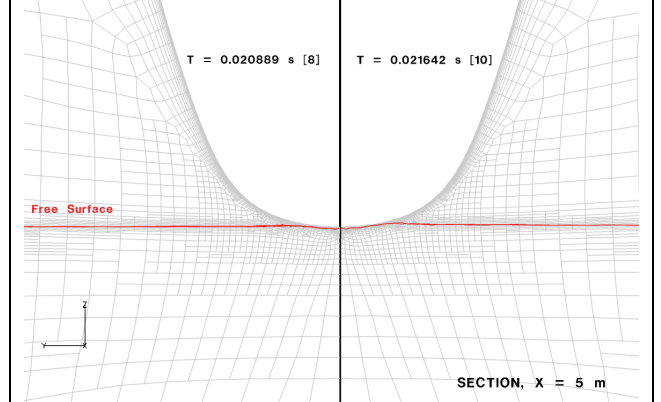


Figure 10: Mesh in the section $X=5\text{m}$, evolution of the refinement from [8] to [10] in phase 1

In the two pictures of figure 8 ($\Delta T = 0.0114$ between the two pictures) we see the illustration of the refinement and derefinement: when refined cells are situated under the free surface they are merged back into the original coarse cells and the mesh is the same as before the refinement.

In the figure 9 ($\Delta T = 0.001$ s) and figure 10 ($\Delta T=0.0007$ s) this is less refinement and derefinement visible between the two pictures, because the delay is shorter and the original mesh is finer behind the hull than on the side of the hull.

We present in figure 11 a view of the deformation of the free surface at $T= 0.0505$ s. We observe on the two sides of the float the development of a breaking wave.

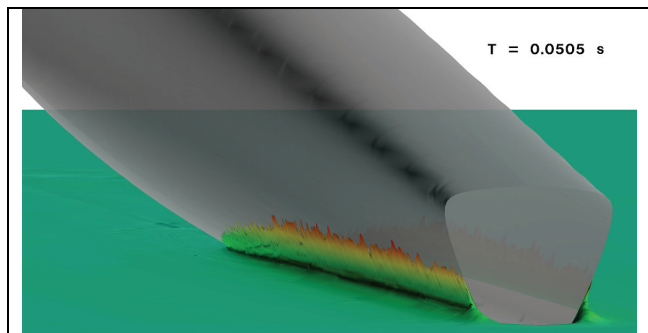


Figure 11: View of the deformation of the free surface at $T=0.0505$ s.

5. CONCLUSIONS

In this paper we presented a new methodology of automatic mesh refinement based on the size of cells for the good description of the free surface.

The new automatic adaptive grid refinement and derefinement method is very well adapted to compute the difficult unsteady phenomenon of impact.

The computed dynamic pressure results have been used by Team Groupama to better understand the phenomenon and to calibrate design methods.

In the future, the new method presented in this paper will serve as an efficient tool for naval architects and engineers to define the extreme load cases applied to yacht structure by the slamming effects. The traditional methods used in the past and the application of linear coefficients to hydrostatic loads in order to quantify slamming effects can now be refined by efficient dynamic methods to improve the knowledge for a boat speed of 30 to 40 knots.

6. ACKNOWLEDGEMENTS

This work was performed using HPC resources from GENCI-IDRIS (Grant2010-x2010021308).

7. REFERENCES

1. DENG, G.B. and VISONNEAU, M. ‘Comparison of explicit algebraic stress models and second-order turbulence closures for steady

flows around ships’, *Proceedings of the 7th International Conference on Numerical Ship Hydrodynamics, Nantes, France*, 1999.

2. DUVIGNEAU, R., VISONNEAU, M. and DENG G.B., ‘On the role played by turbulence closures in hull shape optimisation at model and full scale’, *J. Marine Science and Technology*, Vol. 8, No. 1, pp.1-25, 2003.
3. HAY, A. and LEROYER, A. and VISONNEAU, M., ‘H-adaptive Navier-Stokes simulations of free-surface flows around moving bodies’, *J. Marine Science and Technology*, Vol. 11, No. 1, pp.1-18, 2006.
4. KARYPIS, G. and KUMAR, V., ‘Parallel multilevel k-way partitioning scheme for irregular graphs’, *SIAM Review*, Vol. 41, No. 2, pp.278-300, 1999.
5. LEROYER, A. and VISONNEAU, M., ‘Numerical methods for RANSE simulations of a self-propelled fish-like body’, *J. Fluid & Structures*, Vol. 20, No. 3, pp.975-991 , 2005.
6. MENTER, F.R., ‘Zonal two equation k-omega turbulence models for aerodynamic flows’, *AIAA Paper 93-2906*, 1993.
7. QUEUTEY, P. and VISONNEAU, M., ‘An interface capturing method for free-surface hydrodynamic flows’, *Computers & Fluids*, Vol. 36, No. 9, pp.1481-1510, 2007.
8. WACKERS, J. and VISONNEAU, M., ‘Adaptive grid refinement for free-surface flow computation’, *Proceedings of ECCOMAS MARINE 2009*, 2009.

8. AUTHORS’ BIOGRAPHIES

Yann Roux holds the current position of C.E.O. at company K-Epsilon. He is the funder of the company K-Epsilon. In partnership with laboratory he develops tools and proposes studies in unsteady hydrodynamic and aerodynamic computation.

Jeroen Wackers is Research Engineer in the Fluid Mechanics laboratory at Ecole Centrale de Nantes. He is in charge of the research concerning adaptive and goal-oriented computation for ISIS-CFD.

Loïc Dorez holds the current position of Head of Design Office at Groupama Sailing Team. In partnership with laboratories, design structure compagnies, aerodynamic and hydrodynamic compagnies he organises developpements of tools and shares sailing experience on various subjects apply during the last ten years race multihulls.